

A novel pyrene-2-(pyridin-2-ylmethylsulfanyl)ethylamine based turn-on dual sensor for Al³⁺: experimental and computational studies†

Rahul Bhowmick^a, Malay Dolai^a, Rabiul Alam^a, Tarun Mistri^a, Atul Katarkar^b, Keya Chaudhuri^b and Mahammad Ali^{a*}

Table of contents

1. ¹H NMR spectrum of P, **Fig. S1**
2. ¹H NMR spectrum of PP, **Fig. S2**
3. ¹H NMR spectrum of Al-PP complex, **Fig. S3**
4. Mass spectrum of P in CH₃OH, **Fig. S4**
5. Mass spectrum of PP in CH₃OH, **Fig. S5**
6. Mass spectrum of Al-PP in CH₃OH, **Fig. S6**
7. IR Spectrum of Al-PP complex, **Fig. S7**
8. Naked eye image of PP and corresponding Al³⁺ complex, **Fig. S8**
9. Dynamic light scattering (DLS) plot, **Fig. S9**
10. Emission spectra of PP in different conc., **Fig. S10**
11. Excitation spectra of PP in different emission, **Fig. S11**
12. Limit of detection and limit of quantification calculation using fluorescence and UV-VIS techniques, **Fig. S12**
13. Reversibility Check of the sensor with EDTA, **Fig. S13**
14. Cytotoxicity test of the ligand PP, **Fig. S14**
15. Table of DLS data, **Table. ST1**
16. Selected parameters for the vertical excitation (UV-VIS absorptions) of L; electronic excitation energies (eV) and oscillator strength (f), configurations of the low-lying excited states of L; calculation of the S₀→S_n energy gaps on optimized ground-state geometries (UV-vis absorption), **Table. ST2**
17. Main calculated optical transition for the complex 1 with composition in terms of molecular orbital contribution of the

transition, vertical excitation energies, and oscillator strength in methanol, **Table. ST3**

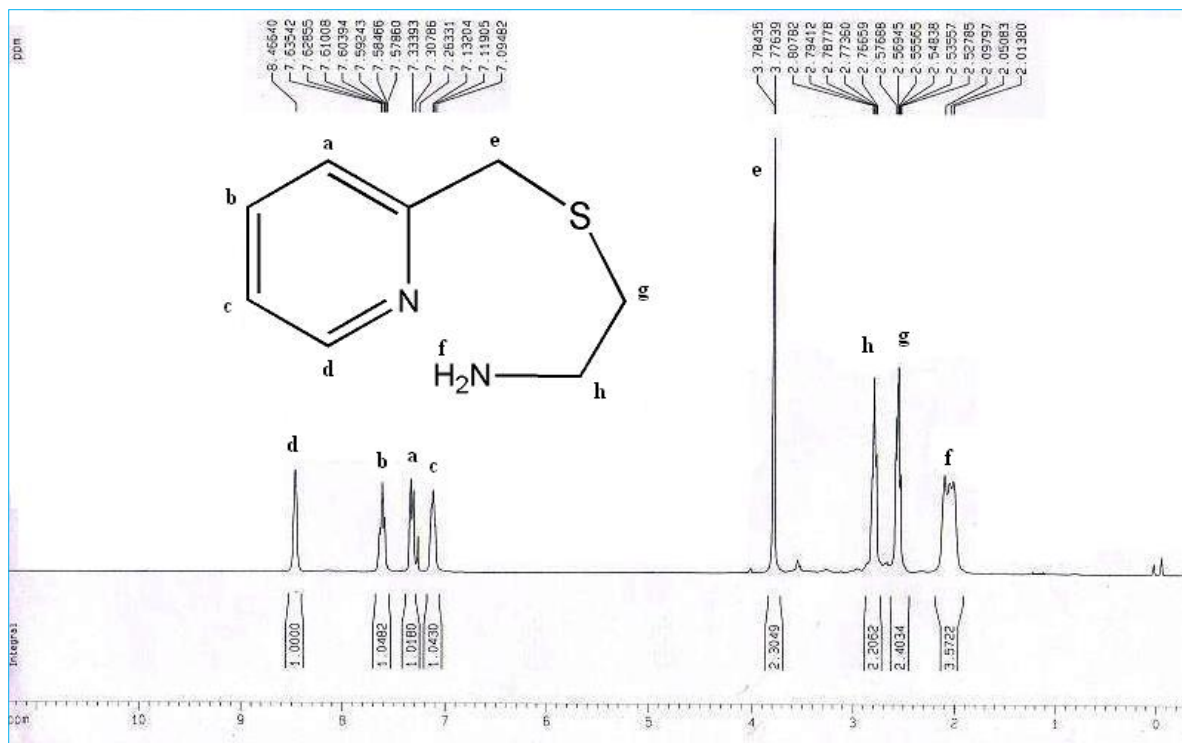


Fig. S1 ^1H NMR spectrum of **P** in CDCl_3 in Bruker 300 MHz instrument.

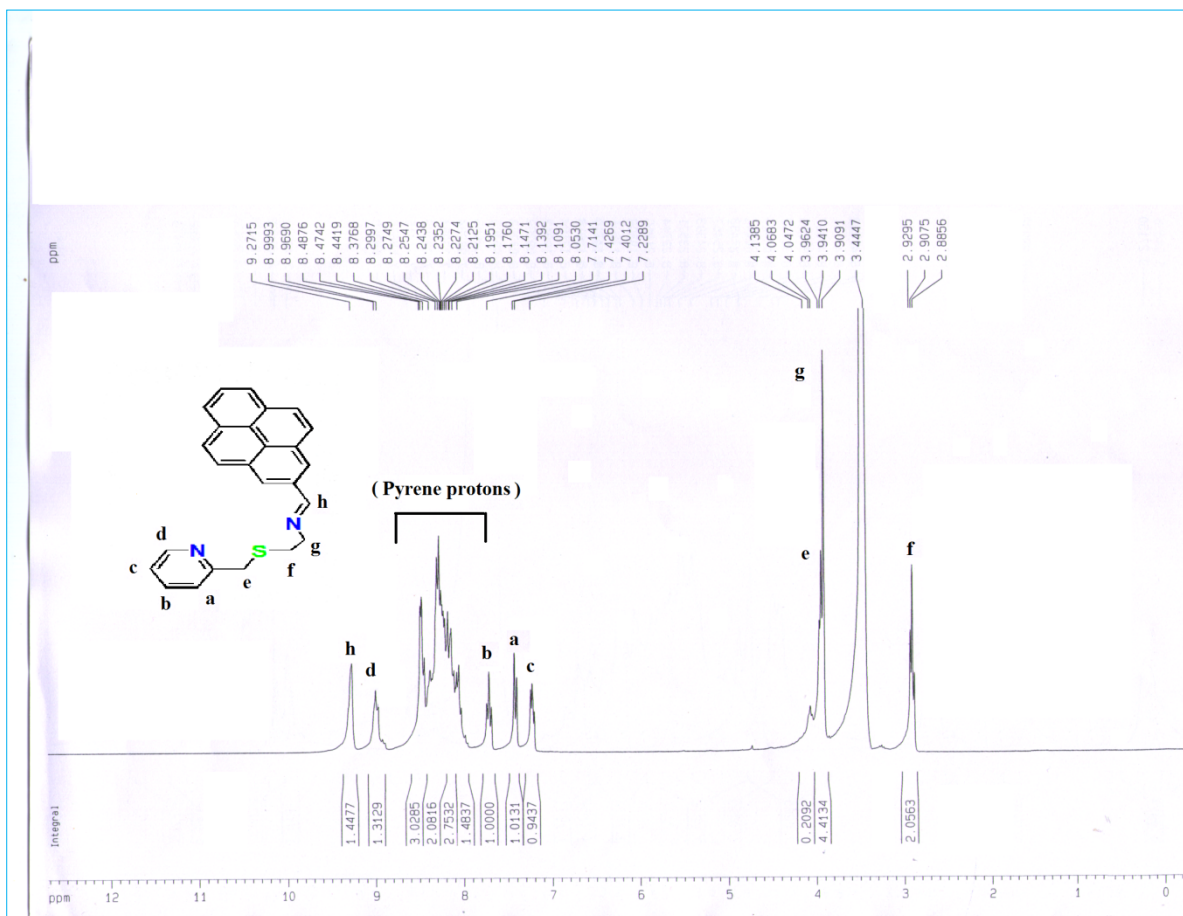


Fig.S2 ^1H NMR spectrum of **PP** in $\text{DMSO}-\text{d}_6$ in Bruker 300 MHz instrument.

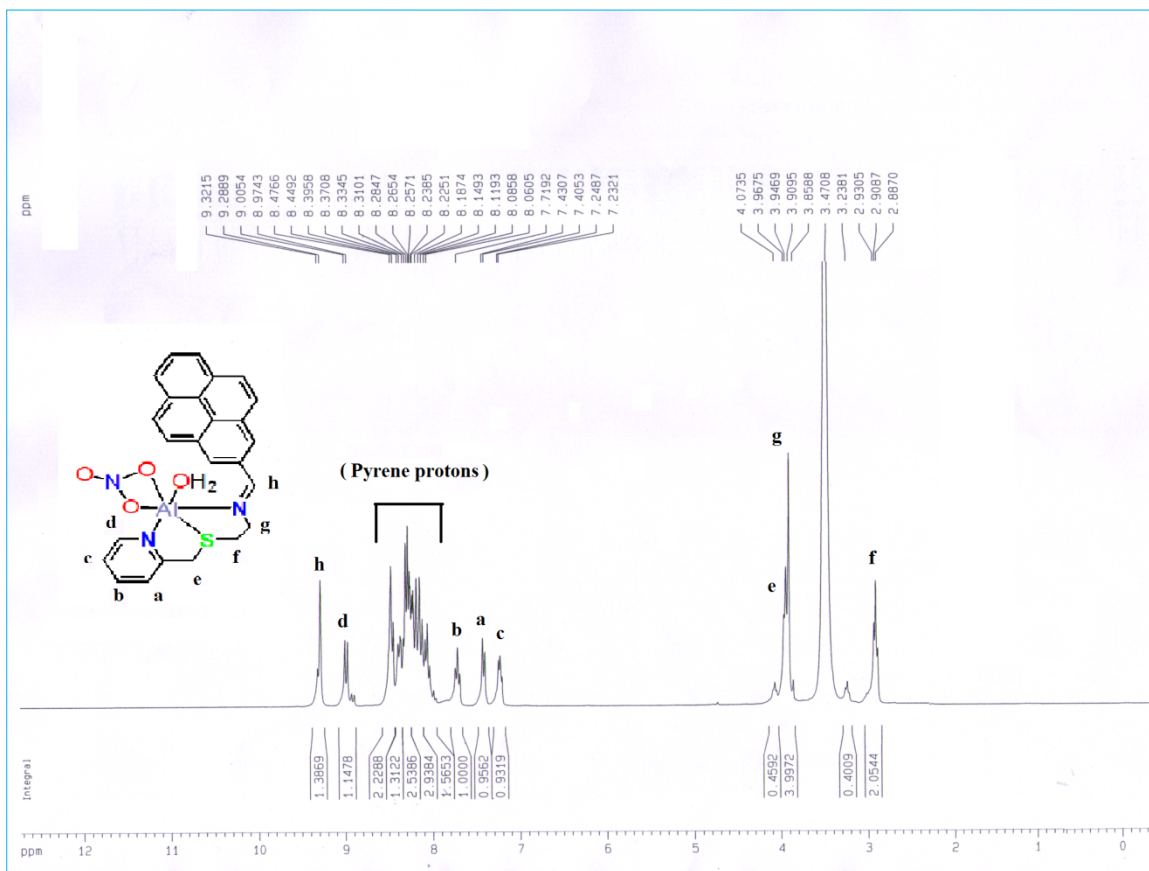


Fig.S3 ^1H NMR spectrum of **PP+** Al^{3+} in DMSO-d_6 in Bruker 300 MHz instrument.

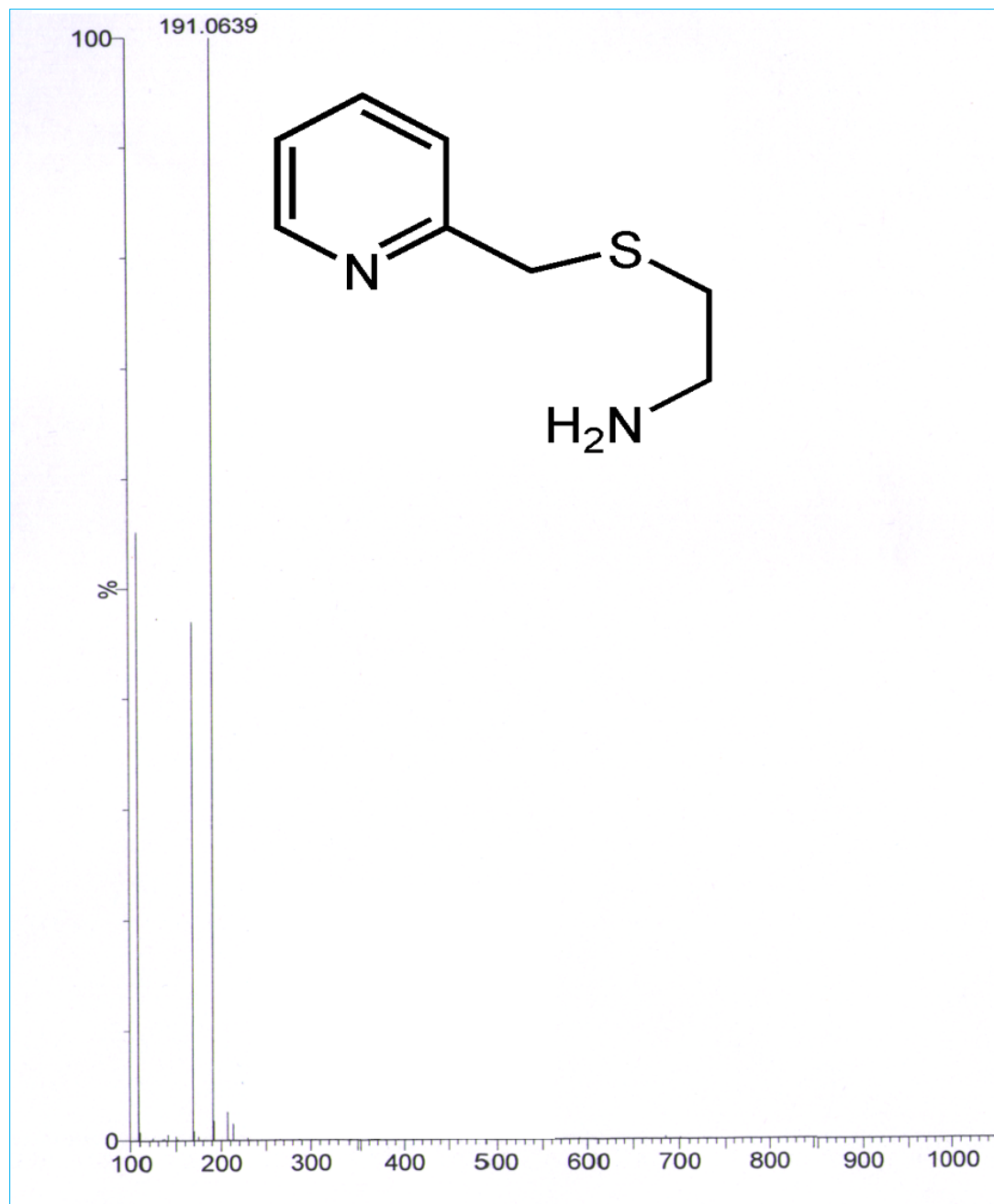


Fig. S4 Mass spectrum of **P** in CH_3OH .

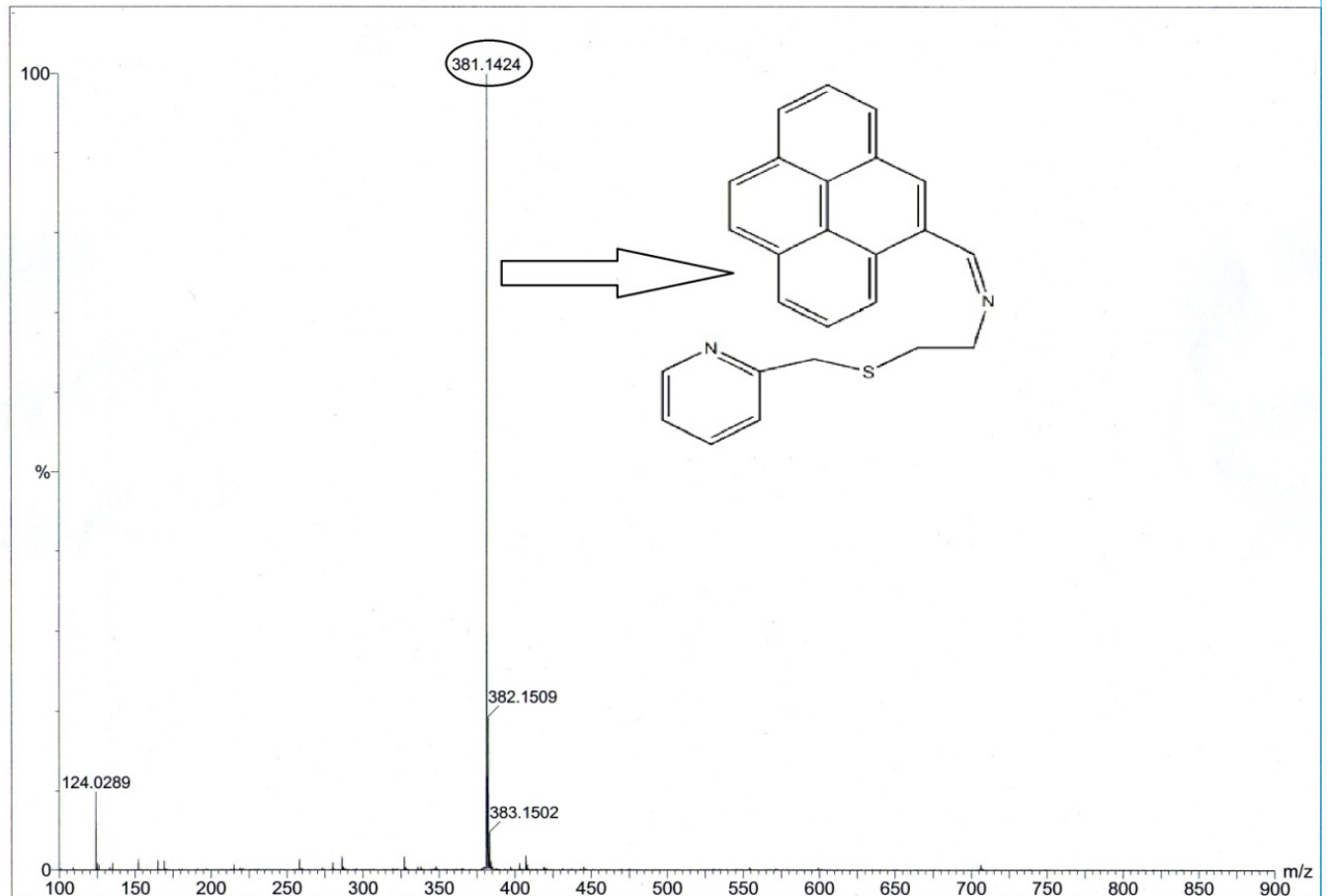


Fig.S5 Mass spectrum of **PP** in CH_3OH .

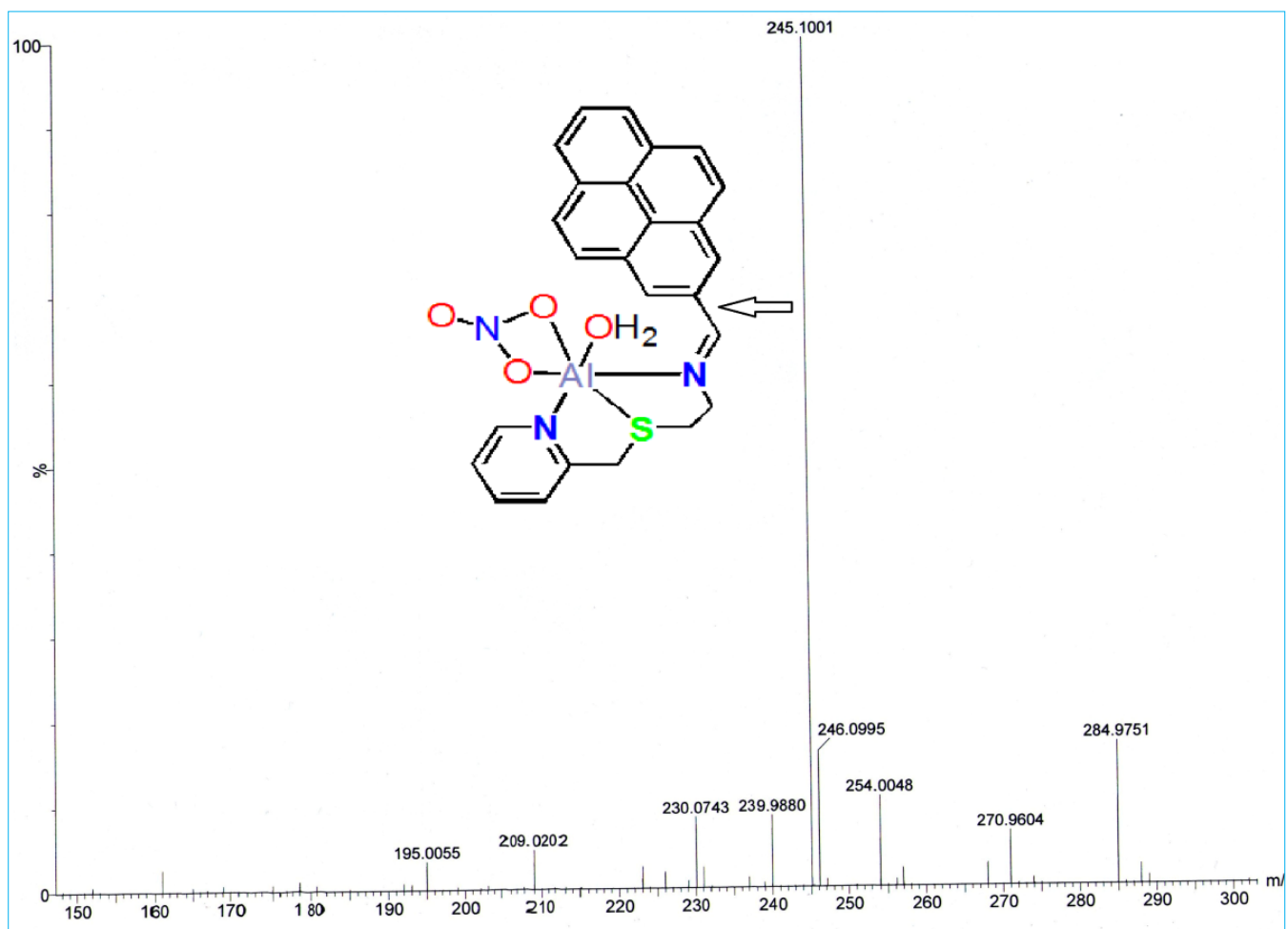


Fig.S6 Mass spectrum of $\text{PP}+\text{Al}^{3+}$ in CH_3OH .

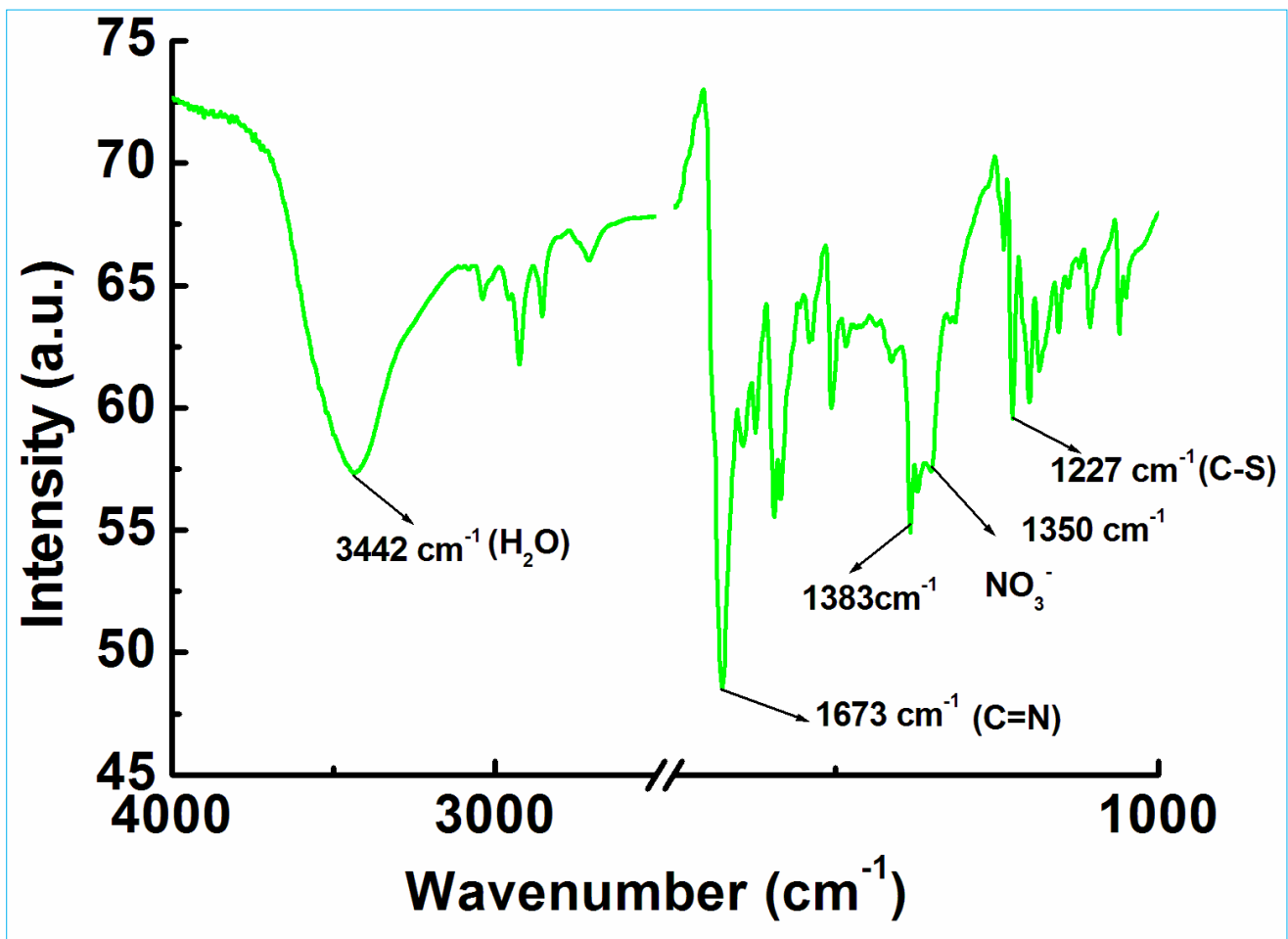


Fig. S7 IR spectrum of Al-PP complex.

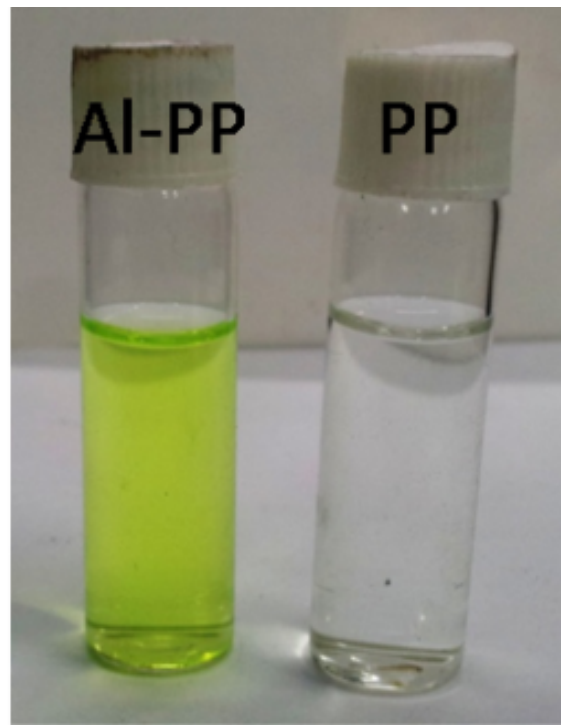
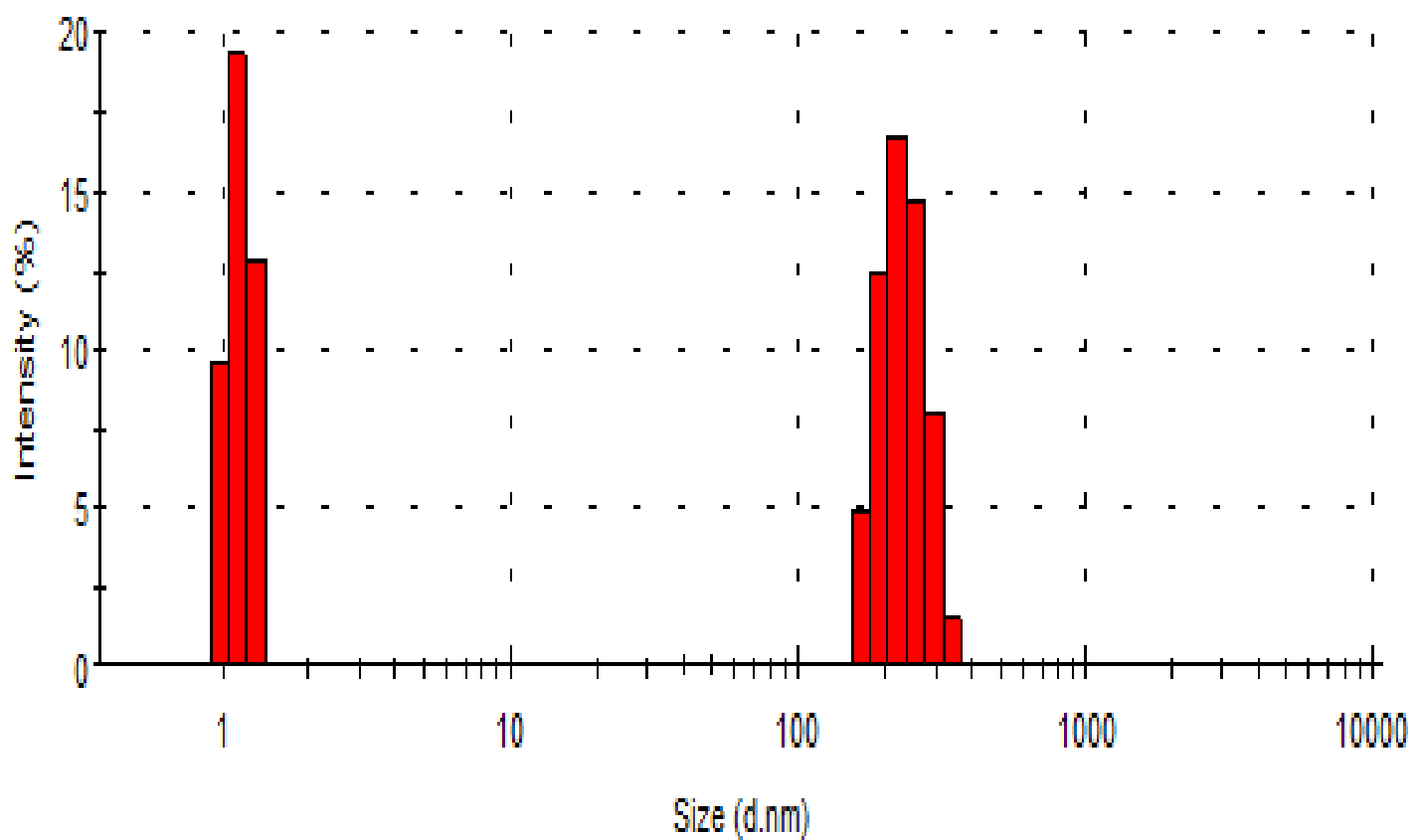


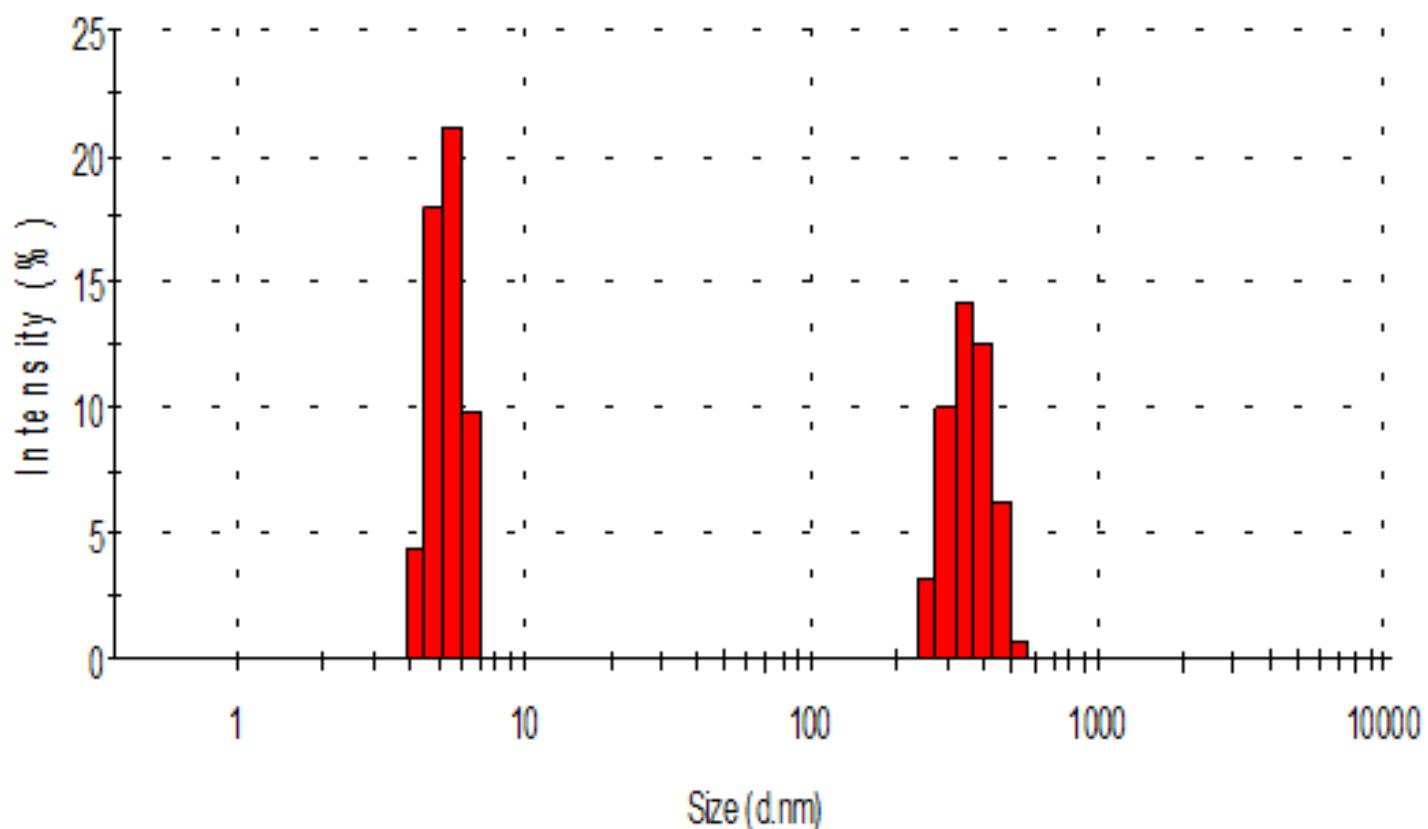
Fig. S8 Naked eye images of PP (20 μM) in presence of equimolar amount of Al^{3+} in aqueous-methanol solution at pH 7.2 (HEPES buffer).

Statistics Graph (1 measurements)



Dynamic light scattering (DLS) plot of PP

Statistics Graph (1 measurements)



Dynamic light scattering (DLS) plot of PP+ Al³⁺

Fig.S9 Dynamic light scattering (DLS) plot.

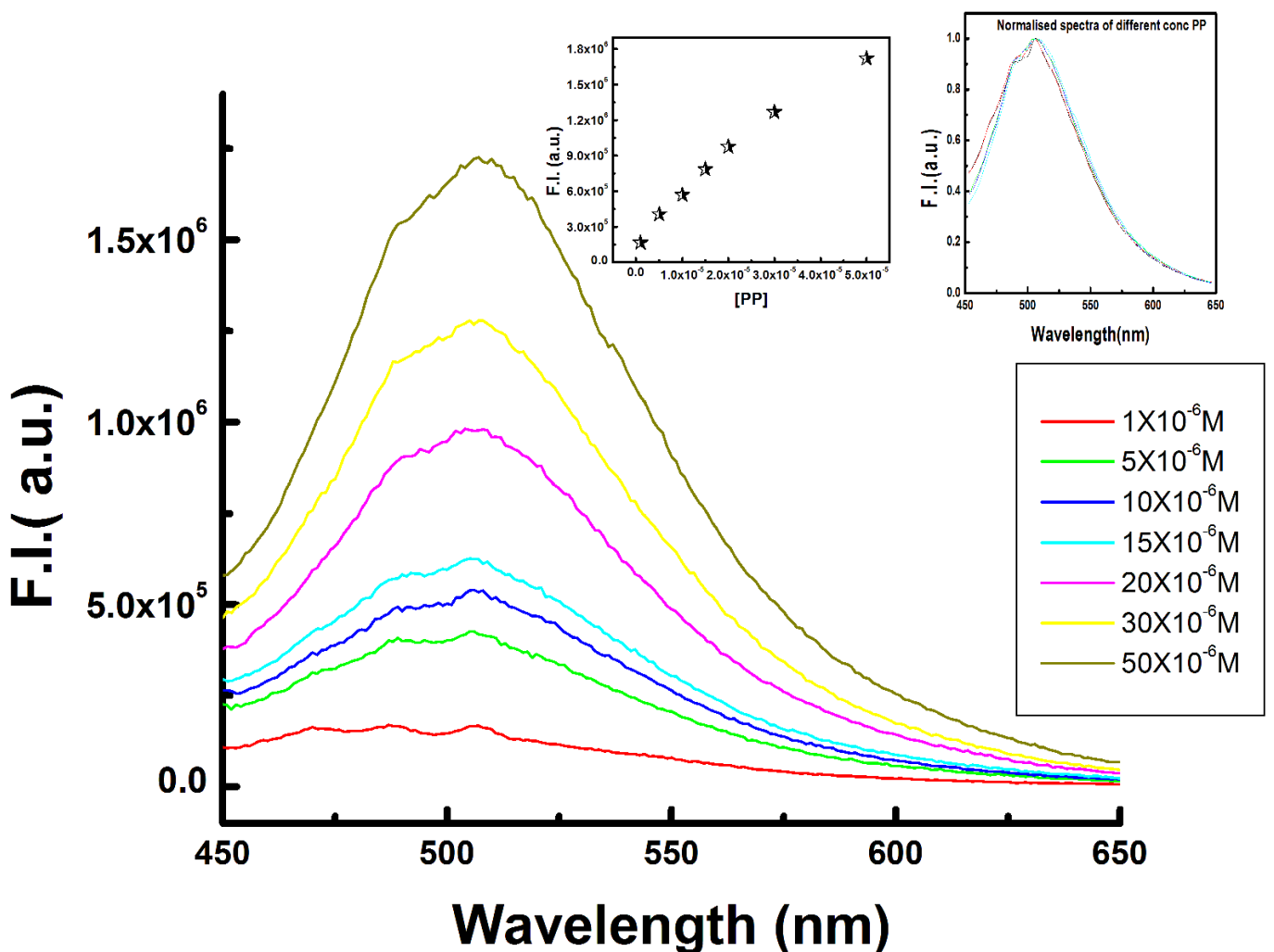


Fig. S10 Emission spectra of PP in different concentrations at $\lambda_{\text{ex}} = 440\text{nm}$ (inset normalised spectra).

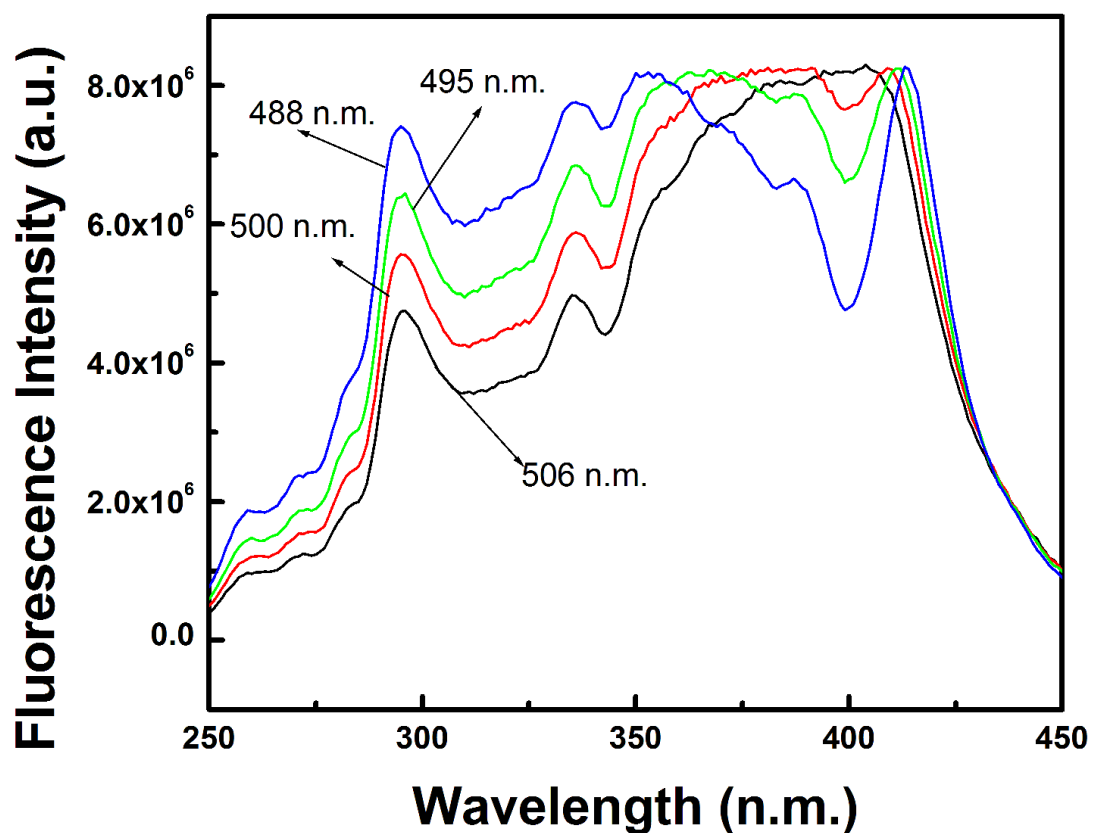
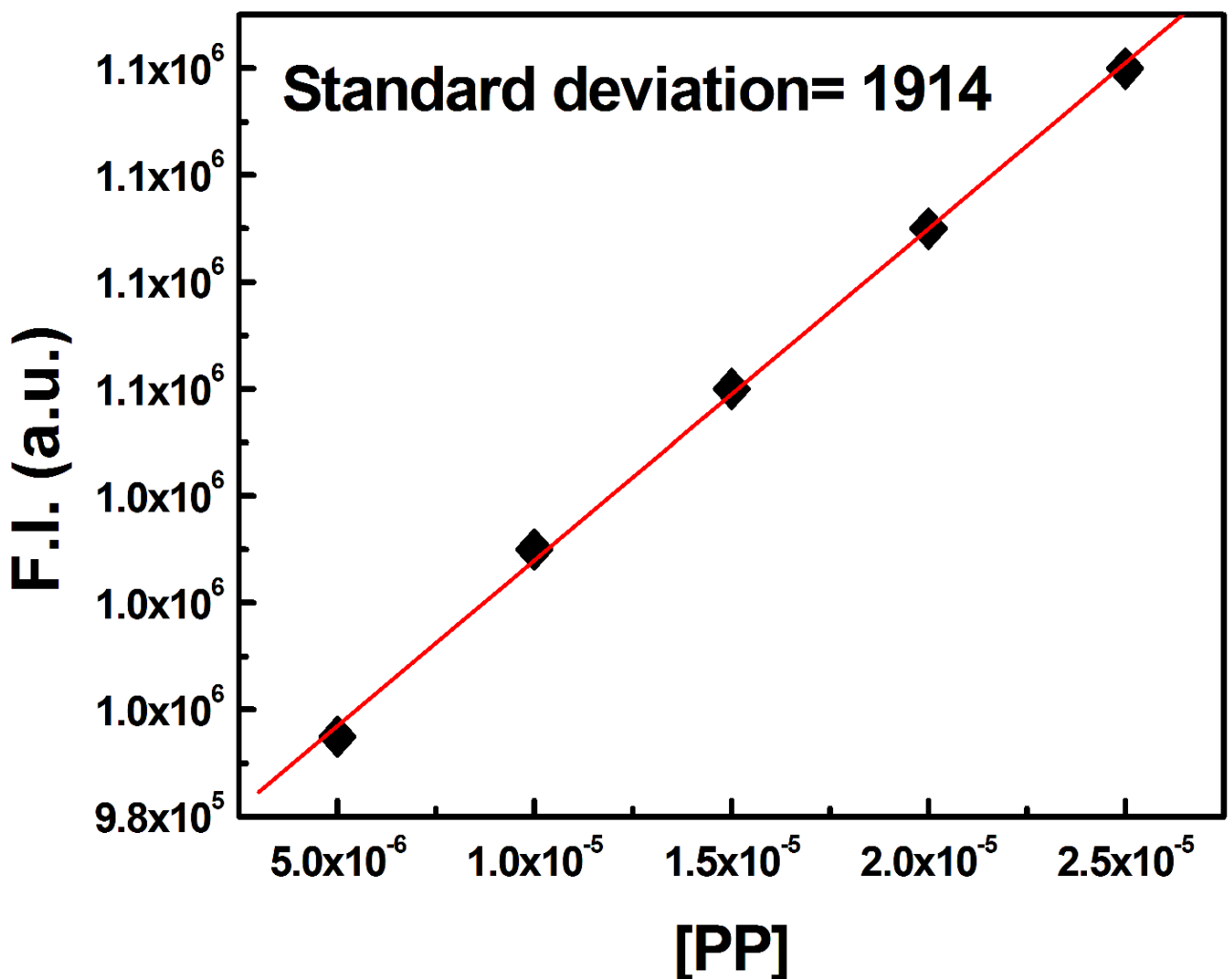
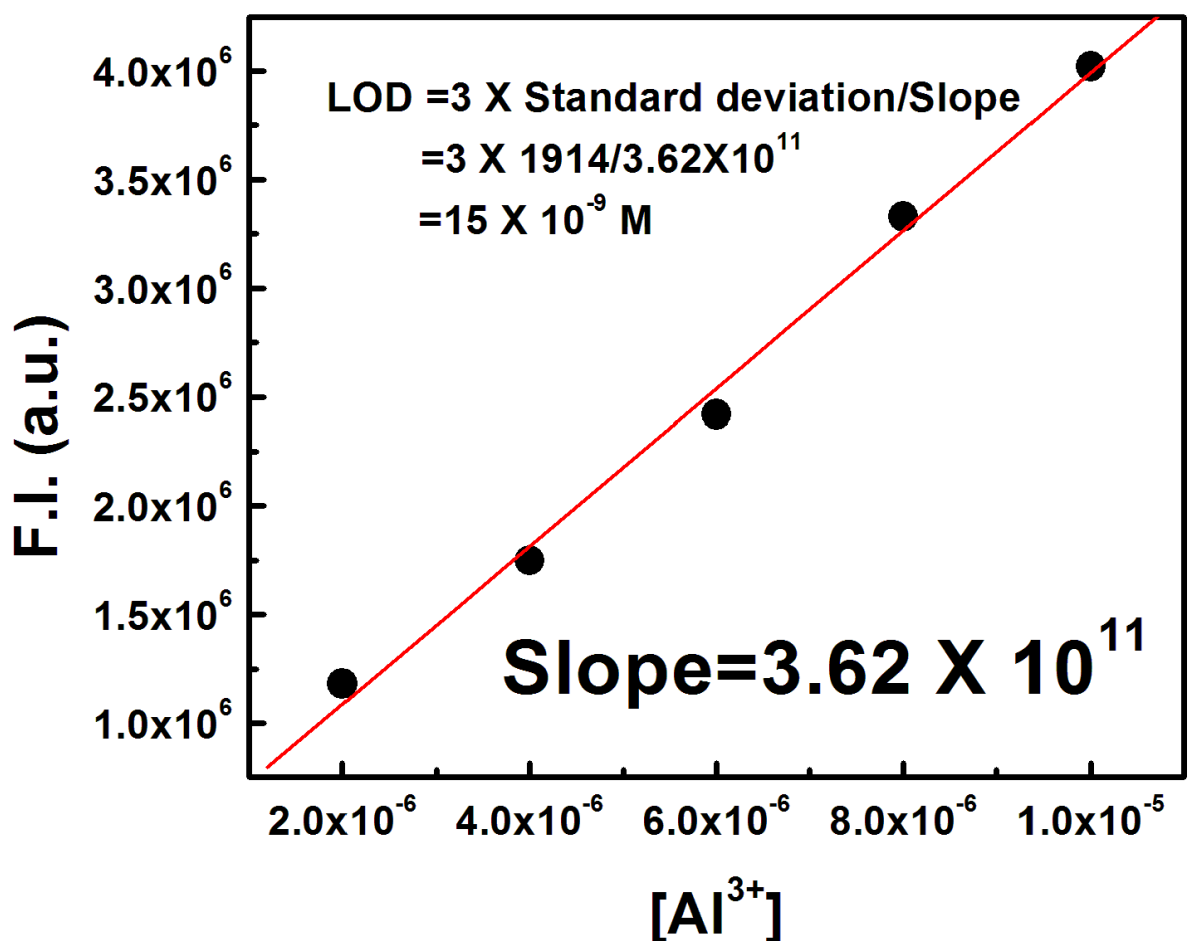


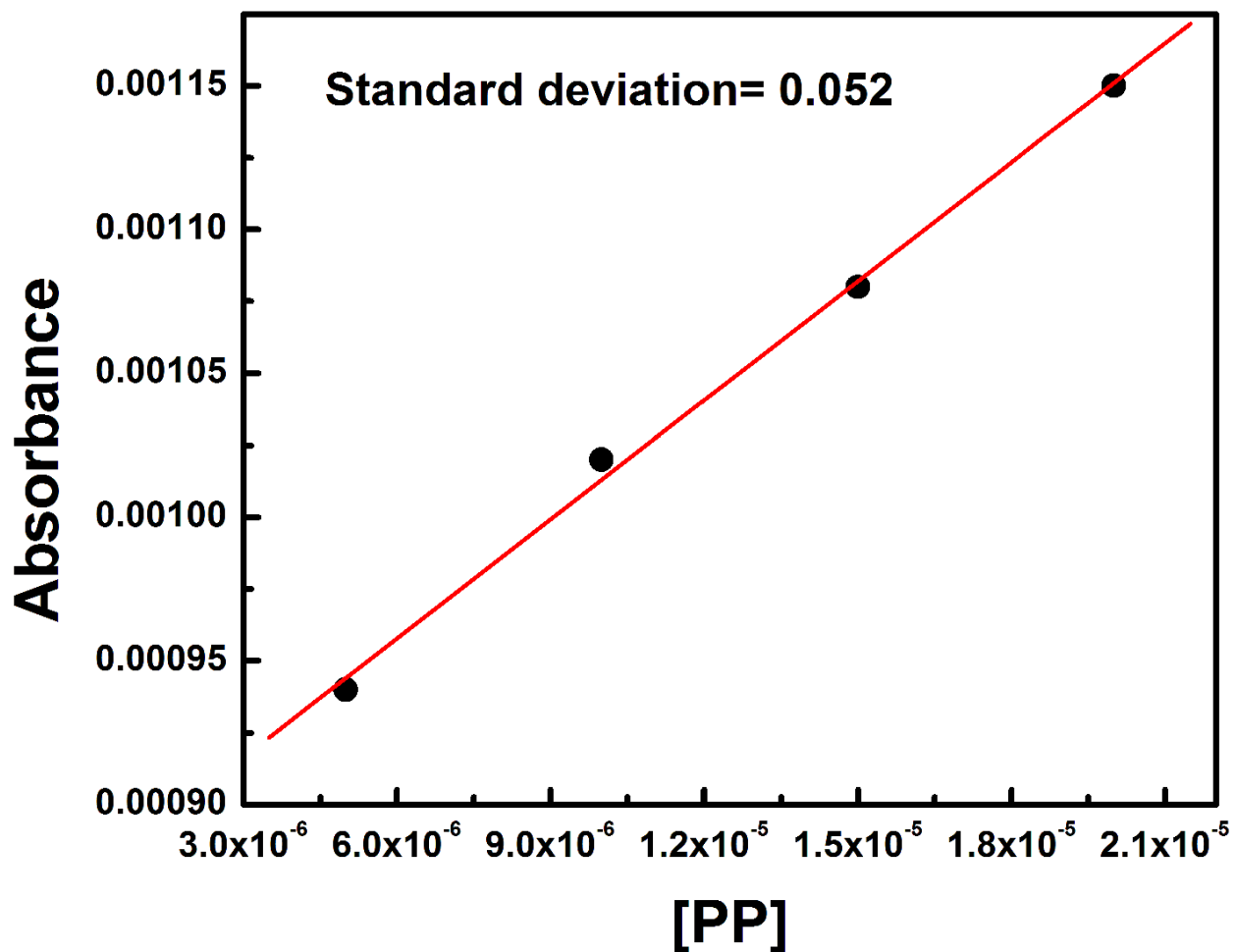
Fig.S11 Excitation spectra of PP in 506, 500, 495 and 488nm emission.

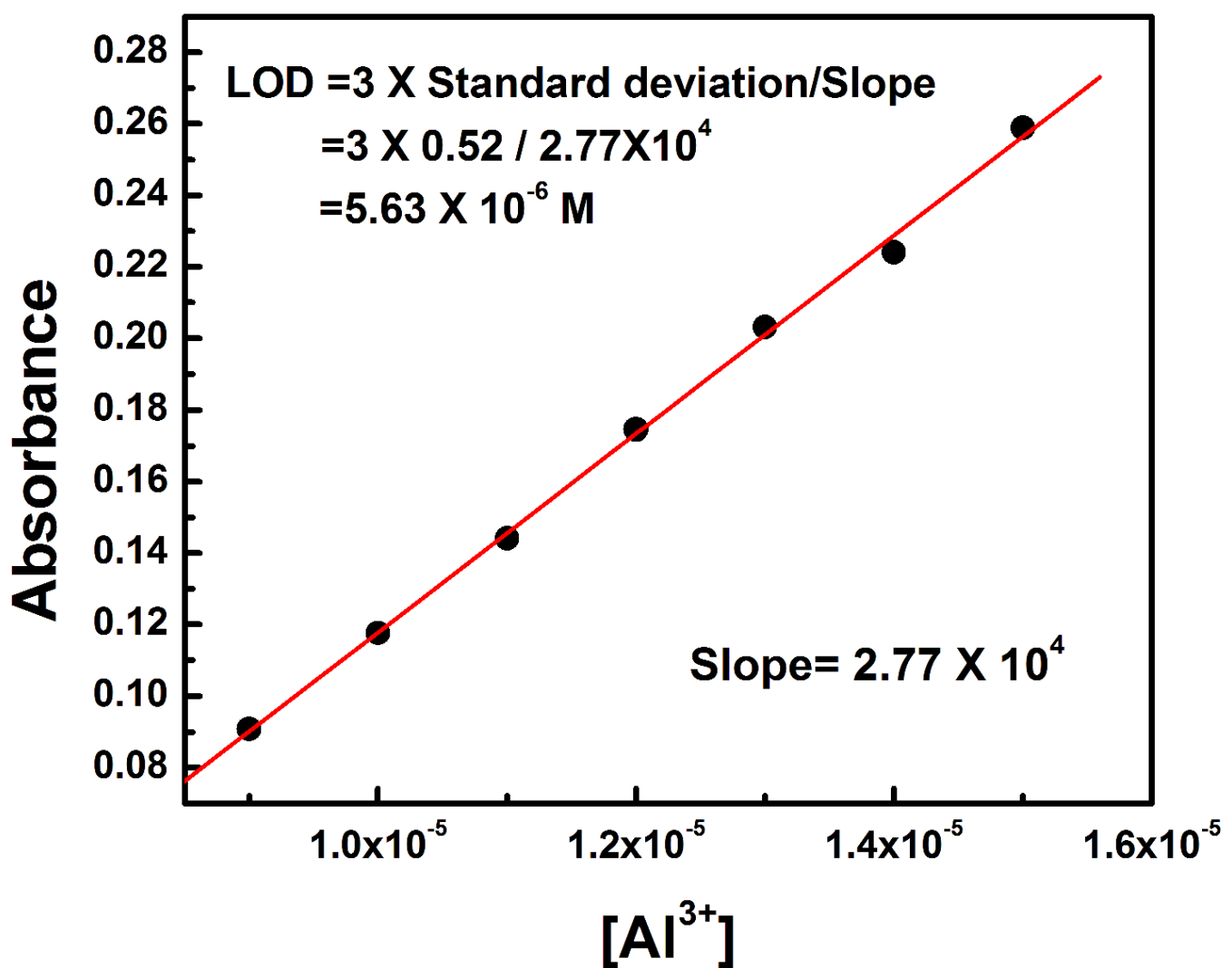




Limit of detection (LOD) plot using fluorescence technique.

Limit of quantification= 10 x Standard deviation of blank/Slope
= 10X 1914 / 3.62X10¹¹
= 5.28 X 10⁻⁸ M





Limit of detection (LOD) plot using UV-VIS technique.

Limit of quantification= 10X Standard deviation of blank / Slope
 $= 10 \times .52 / 2.77 \times 10^4$
 $= 1.87 \times 10^{-4} \text{ M}$

Fig. S12 Limit of detection and limit of quantification plots using fluorescence and UV-VIS techniques.

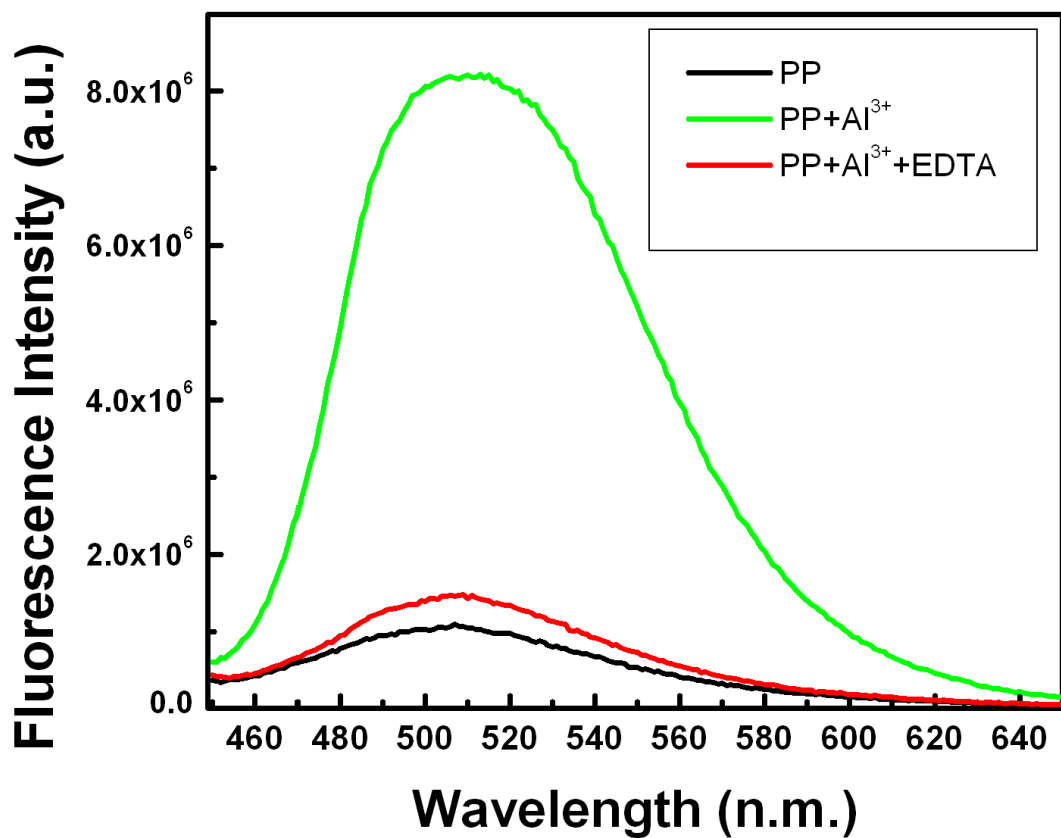


Fig.S13 Reversibility plot with EDTA.

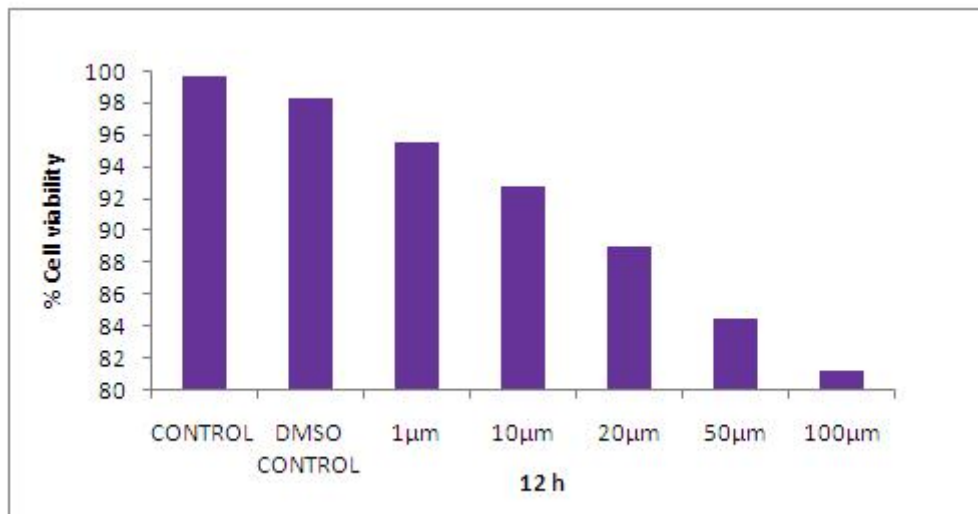


Fig.14 Cytotoxicity test of the ligand PP.

Table S1 Dynamic light scattering (DLS) data of PP and PP+Al³⁺

		Size (d.nm)	% of Intensity	Width (n. nm)
PP	Peak 1	1.137	41.8	42.32
	PEAK 2	231.5	58.2	0.1206
PP+ Al ³⁺	Peak 1	5.402	53.3	0.6838
	Peak 2	358.9	46.7	61.47

Table S2 Selected parameters for the vertical excitation (UV-VIS absorptions) of L; electronic excitation energies (eV) and oscillator strength (f), configurations of the low-lying excited states of L; calculation of the $S_0 \rightarrow S_n$ energy gaps on optimized ground- state geometries (UV-vis absorption).

Electronic transition	Composition	Excitation energy	Oscillator strength (f)	CI	Assignment	λ_{exp} (nm)
$S_0 \rightarrow S_2$	HOMO-2 → LUMO+1	3.9974eV (339nm)	0.3895	0.15137	ILCT	343
	HOMO → LUMO			0.64857	ILCT	
	HOMO → LUMO+1			-0.18792	ILCT	
$S_0 \rightarrow S_7$	HOMO-2 → LUMO	4.2529 eV (291 nm)	0.1511	0.58459	ILCT	286/275
	HOMO → LUMO + 1			0.26132	ILCT	
	HOMO → LUMO + 4			0.21850	ILCT	
$S_0 \rightarrow S_{11}$	HOMO-2 → LUMO+1	4.6548eV (266 nm)	1.2965	0.64553	ILCT	263/260
	HOMO-1 → LUMO + 3			-0.12244	ILCT	
	HOMO → LUMO			-0.14788	ILCT	
$S_0 \rightarrow S_{17}$	HOMO-7 → LUMO +1	5.0265 eV (246 nm)	0.1124	0.10092	ILCT	243/233
	HOMO-2 → LUMO			0.16606	ILCT	
	HOMO → LUMO+5			0.61462	ILCT	

Table S3 Main calculated optical transition for the complex 1 with composition in terms of molecular orbital contribution of the transition, vertical excitation energies, and oscillator strength in methanol.

Electro nic transiti on	Compositi on	Excitatio n energy	Oscillat or strength (f)	CI	Transiti on assigne d	λ_{exp} (nm)
$S_0 \rightarrow S_6$	HOMO – 2 → LUMO+1	3.1468e V (394 nm)	0.3069	- 0.1 139 6	MLCT/IL CT	390
	HOMO – 1 → LUMO+1		0.6550	6	MLCT/IL CT	
	HOMO → LUMO + 3			- 0.2 334 8	ILCT	
$S_0 \rightarrow S_8$	HOMO – 2→ LUMO + 1	3.4719e V (357 nm)	0.0405	0.69131	MLCT/IL CT	360
	HOMO – 1→ LUMO + 1		0.11297		MLCT/IL CT	
$S_0 \rightarrow S_{11}$	HOMO – 4→ LUMO + 1	3.7093e V (334nm)	1.3617	0.14673	MLCT/IL CT	343
	HOMO – 1→ LUMO + 1		0.23355		MLCT/IL CT	
	HOMO → LUMO + 3		0.62749		ILCT	

